Theoretical Studies of Regioselectivity in the Photochemical Cycloaddition of Allene to Cyclopentenone

Robert D. J. Froese, Gordon L. Lange, and John D. Goddard*

Guelph-Waterloo Centre for Graduate Work in Chemistry, Department of Chemistry and Biochemistry, University of Guelph, Guelph, Ontario, Canada N1G 2W1

Received July 28, 1995[⊗]

In the photocycloaddition of allene to cyclopentenone, four different triplet 1,4-biradicals can form, two of which contain an allylic moiety from addition to the central carbon of allene, while two others result from addition to a terminal carbon of the allene. The two biradicals containing the allyl fragment are predicted to be approximately 20 kcal/mol lower in energy than the other two. Using a model for the reaction mechanism in which the relaxed triplet excited state of allene reacts with ground state cyclopentenone, the reaction barriers to forming these allylic substituted systems are lower by *ca.* 8−10 kcal/mol in comparison to the other two. The conformation of the biradicals upon spin inversion is in all probability one important factor in determining whether the biradicals close to products or revert to starting materials. The sp^3 hybridization at the bond-forming carbon in the vinyl (nonallylic) systems leads to nearly free rotation about that bond, and three shallow minima and the corresponding transition states for internal rotation were located. One minimum has the two carbon centers which carry the excess spin density about 3.8 Å, apart while in the other two minima the distances are ∼3.1 Å. Taking these distances into account, it is estimated that very few of the intermediates formed from the addition α to the carbonyl close to products. In contrast, a high percentage of the systems formed from attack β to the carbonyl are predicted to yield products. In the allylic substituted systems, carbon centers with some radical character are always relatively close to the site of radical character in the cyclopentenone ring. The relative ratio of cycloadducts can be estimated from the distribution of the biradicals. Important factors considered in this study include energetics, conformations, spin−orbit coupling constants, and the singlet−triplet energy splittings of the intermediate biradicals.

Introduction

Photochemical [2 + 2] cycloadditions are very important in synthetic organic chemistry and especially in the synthesis of natural products.[1,2] A model for enone cycloaddition to an alkene involving an excited state complex was first proposed by Corey[3] and later modified by de Mayo.[4,5] Originally, it was suggested that the lowest triplet state of the enone was n,π*, and this excited species reacted with an alkene to generate a triplet exciplex. Now, it generally assumed[6] that a π,π* triplet enone reacts with an alkene to form a triplet 1,4-biradical, which after spin inversion closes to products.

In the addition of an asymmetrical olefin to an α,β-unsaturated ketone, there are two regioisomers, the head-to-head (HH) and head-to-tail (HT) adducts, where head refers to the carbonyl end of the enone and to the more substituted end of the olefin. For each regioisomer, there are various possible stereoisomers. Corey[2,3] was the first to suggest that for electron-rich alkenes, the substituent on the alkene will orient itself away from the carbonyl of the enone (head-to-tail). This concept follows from the reversal of the dipole moment in the enone n,π* excited state. The orientation of the addition is influenced by dipole−dipole interactions, and solvent effects should be important.[7] To maximize the effects proposed in Corey's model, a nonpolar solvent should be used.[7−9] There remain numerous experimental contradictions to the hypothesis. Two studies indicated that additions to cyclopentenone and cyclohexenone rings lead predominantly to head-to-head addition.[10−12] The addition of methyl 1-cyclobutene-1-carboxylate to substituted cyclic enones[13−16] leads mostly to the head-to-head product. A series of experiments compared regioselectivities in the addition of 3-methyl-2-cyclohexenone to three alkenes: methyl 1-cyclobutene-1-carboxylate, methyl 1-cyclopentene-1-carboxylate, and methyl 1-cyclohexene-1-carboxy-

⊗ Abstract published in *Advance ACS Abstracts,* January 1, 1996.

(1) (a) Baldwin, S. W. *Organic Photochemistry*; Padwa, A., Ed.; Dekker: New York, 1981; Vol 5., pp 123−225. (b) Oppolzer, W. *Acc. Chem. Res.* **1982**, *15*, 135. (c) Weedon, A. C. *Synthetic Organic Photochemistry*; Horspool, W. M., Ed.; Plenum: New York, 1984; pp 61−144. (d) Schuster, D. I. *Chemistry of Enones*; Patai, S., Rappoport, Z., Eds.); Wiley: New York, 1989; pp 623−756. (e) De Keukeleire, D.; He, S.-L. *Chem. Rev.* **1993**, *93*, 359. (f) *CRC Handbook of Organic Photochemistry and Photobiology*; Horspool, W. M., Song, P.-S., Eds.; CRC Press: Boca Raton, FL, 1995; Chapters 52 and 53.

(2) (a) Becker, D.; Haddad, N. *Organic Photochemistry*; Padwa, A., Ed.; Dekker: New York, 1989; Vol. 10, pp 1−162. (b) Crimmins, M. T. *Chem. Rev.* **1988**, *88*, 1453.

(3) (a) Corey, E. J.; Nozoe, S. *J. Am. Chem. Soc.* **1964**, *86*, 1652. (b) Corey, E. J.; Bass, J. D.; LeMahieu, R.; Mitra, R. B. *J. Am. Chem. Soc.* **1964**, *86*, 5570.

(4) de Mayo, P. *Acc. Chem. Res.* **1970**, *4*, 41. Loutfy, R. O.; de Mayo, P. *J. Am. Chem. Soc.* **1977**, *99*, 3559.

(5) Turro, N. J. *Modern Molecular Photochemistry*; Benjamin/Cummings: Menlo Park, CA, 1978; p 293.

(6) Schuster, D. I.; Heibel, G. E.; Brown, P. B.; Turro, N. J.; Kumar, N. V. *J. Am. Chem. Soc.* **1988**, *110*, 8261.

(7) Challand, B. D.; de Mayo, P. *J. Chem. Soc., Chem. Commun.* **1968**, 982.

(8) Kirkwood, J. G. *J. Chem. Phys.* **1934**, *2*, 351. Onsager, L. *J. Am. Chem. Soc.* **1936**, *58*, 1486.

(9) Berenjian, N.; de Mayo, P.; Sturgeon, M. E.; Sydnes, L. K.; Weedon, A. C. *Can. J. Chem.* **1982**, *60*, 425.

(10) Carless, H. A. J. *J. Chem. Soc., Perkin Trans. 2,* **1974**, 834.

(11) Challand, B. D.; Hikino, H.; Kornis, G.; Lange, G. L.; de Mayo, P. *J. Org. Chem.* **1973**, *38*, 2117.

(12) Williams, J. R.; Callahan, J. R. *J. Chem. Soc., Chem. Commun.* **1979**, 404.

(13) Williams, J. R.; Callahan, J. F. *Synth. Commun.* **1981**, *11*, 551.

(14) Lange, G. L.; McCarthy, F. C. *Tetrahedron Lett.* **1978**, 4749.

(15) Wender, P. A.; Lechleiter, J. C. *J. Am. Chem. Soc.* **1977**, *99*, 267.

(16) Wender, P. A.; Lechleiter, J. C. *J. Am. Chem. Soc.* **1978**, *100*, 4321.

0022-3263/96/1961-0952$12.00/0

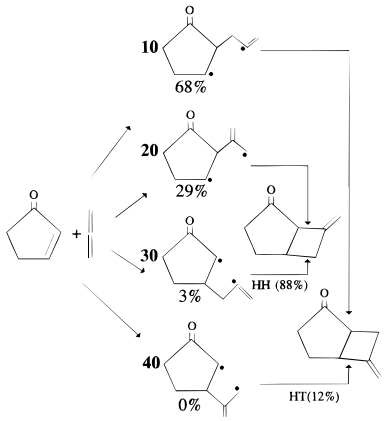

Figure 1. A diagram summarizing Weedon's interpretation of the trapping experiments.[18]

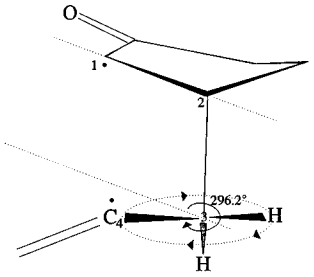

Figure 2. An illustration of nearly free rotation about the C_2-C_3 bond. In this example, the distance between the carbons which carry most of the radical character is 3.072 Å, while the torsional angle is 296.2°. This particular figure depicts biradical **30**.

late.[17] The stereochemistry of the products is *cis*−*anti*−*cis*, but there is a reversal of regioselectivity upon going from the cyclobutene to the cyclohexene rings. The substituted cyclobutene adds >95% head-to-head, cyclopentene results are 50:50, and cyclohexene results are 89% head-to-tail.

The results of studies of regiochemistry in photocycloadditions by Weedon[18−20] are summarized in Figure 1. Weedon postulated that in the addition of allene to cyclopentenone, the relative amounts of the four triplet 1,4-biradicals could be determined by trapping experiments using H_2Se. In these trapping experiments, biradical **10** formed 68% of the intermediates, while biradicals **20**, **30**, and **40** arose 29%, 3%, and 0%, respectively. This data indicates that addition at the α-position of the enone is overwhelmingly favored. Also in contrast to the exciplex model which depends on the relative amounts of the various biradicals, the product distributions were interpreted as depending on the competition of the particular biradicals between reversion to reactants and closure to products. In particular, since the biradicals have nearly free rotation about the single bond shown in Figure 2, the conformation of the triplet biradical upon spin inversion should be an important factor in determining whether the molecule will close to products or revert to starting materials.

Recent theoretical evidence using acrolein as a model enone[21] suggested that differences in the energetics between α- and β-attack can be used to rationalize the ratio of HH and HT products. *Ab initio* studies[21] of the addition of various alkenes, including allene, to acrolein predicted the relative rates of formation of the head-to-head and head-to-tail products.

In the present theoretical study, regioselectivity is examined in the photochemical cycloaddition of allene to cyclopentenone.[20] The energies and geometries of triplet transition states leading to the four triplet 1,4-biradicals from cyclopentenone and triplet allene have been determined. For each of the four triplet biradical minima, conformational isomers were examined. Comparisons of the energies of the two different cycloadducts, HH and HT, were also made. Predictions involved full geometry optimizations at the Hartree−Fock level using the 6-31G* basis set and energy refinement with Møller−Plesset perturbation theory to third order. A comparison of the predicted relative energies and populations of the various minima and transition states should determine which conformations are possible and which reaction pathways are most probable. In addition, spin−orbit coupling constants of which we have calculated the larger one-electron components must be a factor in determining which of the triplet biradicals are likely to convert to singlet biradicals. The computed singlet/triplet energy gap is also important in this regard.

Computational Methods

Ab initio predictions were made with the GAUSSIAN 92[22a] and GAMESS[22b,c] programs employing Silicon Graphics workstations. The 6-31G and 6-31G* basis sets[23] were used for all predictions. Both unrestricted Hartree−Fock[24] and restricted open shell Hartree−Fock methods with the 6-31G* basis set were used for the triplet biradicals. Stationary points were located with analytic energy gradient methods and the algorithms of Schlegel.[25a] These stationary points were then evaluated by determining the harmonic vibrational frequencies using analytic second-derivative[25b] methods and determined to be minima or transition states. These species also were examined including electron correlation, namely unrestricted Møller−Plesset perturbation theory to second or third order (UMP2 or UMP3)[26] and spin-projected Møller−Plesset perturbation theory to second order (PMP2). Single-point energy predictions at the MP levels were

(17) (a) Lange, G. L.; Organ, M. G.; Lee, M. *Tetrahedron Lett.* **1990**, *31*, 4689. (b) Tada, M.; Nieda, Y. *Bull. Chem. Soc. Jpn.* **1988**, *61*, 1416.

(18) Maradyn, D. J.; Sydnes, L. K.; Weedon, A. C. *Tetrahedron Lett.* **1993**, *34*, 2413.

(19) Rudolph, A.; Weedon, A. C. *Can. J. Chem.* **1990**, *68*, 1590.

(20) (a) Hastings, D. J.; Weedon, A. C. *J. Am. Chem. Soc.* **1991**, *113*, 8525. (b) Andrew, D.; Hastings, D. J.; Oldroyd, D. L.; Rudolph, A.; Weedon, A. C. *Pure Appl. Chem.* **1992**, *64*, 1327. (c) Krug, P.; Rudolph, A.; Weedon, A. C. *Tetrahedron Lett.* **1993**, *34*, 7221.

(21) Broeker, J. L.; Eksterowicz, J. E.; Belk, A. J.; Houk, K. N. *J. Am. Chem. Soc.* **1995**, *117*, 1847.

(22) Frisch, M. J.; Trucks, G. W.; Head-Gordon, M.; Gill, P. M. W.; Wong, M. W.; Foresman, J. B.; Johnson, B. G.; Schlegel, H. B.; Robb, M. A.; Replogle, E. S.; Gomperts, R.; Andres, J. L.; Raghavachari, K.; Binkley, J. S.; Gonzalez, C.; Martin, R. L.; Fox, D. J.; Defrees, D. J.; Baker, J.; Stewart, J. J. P.; Pople, J. A. *GAUSSIAN 92, Revision B*; Gaussian, Inc.: Pittsburgh, PA, 1992. (b) GAMESS: Schmidt, M. W.; Baldridge, K. K.; Boatz, J. A.; Elbert, S. T.; Gordon, M. S.; Jensen, J. H.; Koseki, S.; Matsunaga, N.; Nguyen, K. A.; Su, S. J.; Windus, T. L. (c) Dupuis, M.; Montgomery, J. A. *J. Comput. Chem.* **1993**, *14*, 1347.

(23) (a) Hehre, W. J.; Ditchfield, R.; Pople, J. A. *J. Chem. Phys.* **1972**, *56*, 2257. (b) Francl, M. M.; Pietro, W. J.; Hehre, W. J.; Binkley, J. S.; Gordon, M. S.; DeFrees, D. J.; Pople, J. A. *J. Chem. Phys.* **1982**, *77*, 3654. (c) Hariharan, P. C.; Pople, J. A. *Theor. Chim. Acta* **1973**, *28*, 213.

(24) (a) Hartree, D. R. *Proc. Cambridge Philos. Soc.* **1928**, *24*, 89, 111, 246. (b) Fock, V. *Z. Phys.* **1930**, *61*, 126. (c) Roothaan, C. C. J. *Rev. Mod. Phys.* **1951**, *23*, 69. (d) Pople, J. A.; Nesbet, R. K. *J. Chem. Phys.* **1954**, *22*, 571.

(25) (a) Schlegel, H. B. *J. Comput. Chem.* **1982**, *3*, 214. (b) Pople, J. A.; Krishnan, R.; Schlegel, H. B.; Binkley, J. S. *Int. J. Quantum Chem., Symp.* **1979**, *13*, 225.

(26) Møller, C.; Plesset, M. S. *Phys. Rev.* **1934**, *46*, 618.

carried out at the SCF-optimized geometries. Unless otherwise stated, energies and energy differences in this paper are at the UMP3/6-31G*//SCF/6-31G* + ΔZPVE level. The relative populations were found from the equilibrium constants by the thermodynamic relation $\Delta G = -RT \ln K$. The value of ΔG is determined from $\Delta H - T\Delta S$, where ΔH is the enthalpy difference at the UMP3//SCF + ΔZPVE level, T is assumed to be 298.15 K, and ΔS is the total gas-phase entropy difference between the species of interest. In the thermodynamic relationship between internal energy and enthalpy, there is an additional $\Delta(PV)$ term, but in the ideal gas approximation, this $\Delta(PV) = \Delta n(RT)$ term can be neglected as long as we do not compare the reactants ($n = 2$) with an intermediate ($n = 1$). For selected transition states, intrinsic reaction coordinates were followed at the 6-31G* SCF level to ensure which minima were connected by the reaction path. To determine the likelihood of intersystem crossings, the one-electron components of the spin−orbit coupling constants were calculated by the method of Furlani and King.[27] A complete active space SCF (CAS-SCF) method was used for both the triplet and the singlet states with the core orbitals frozen and taken from the triplet wave function. In this case, there were 28 frozen core orbitals from a UHF/6-31G calculation, and there were 10 electrons and 10 orbitals in the active space, i.e., a CAS(10,10). The energy difference between the singlet and triplet biradicals also was considered important. A comparison of CAS(10,10)/6-31G singlet and triplet state energies gives a reasonable estimate of the splitting between the two potential energy surfaces.

Results and Discussion

Reactants. The adiabatic excitation energies from the ground electronic state to the lowest two excited triplet states for cyclopentenone are important to our analysis. At the MP3/6-31G*//SCF/6-31G* + ΔZPVE level of theory, the predicted ground state singlet to triplet energy differences for cyclopentenone are 72.3 kcal/mol for the $\pi \rightarrow \pi^*$ excitation (in Table 2, the difference between **3** and **5**) and 74.3 kcal/mol for the $n \rightarrow \pi^*$ state (**3** and **4**). This predicted value compares very favorably with the experimental $S_0 \rightarrow T_1$ energy of *ca.* 73 kcal/mol for cyclopentenone determined using photoacoustic calorimetry.[28]

The predicted geometries of the possible reactants including ground singlet state allene (**1**), triplet allene (**2**), ground singlet state cyclopentenone (**3**), triplet $n \rightarrow \pi^*$ (**4**), and triplet $\pi \rightarrow \pi^*$ (**5**) cyclopentenone are shown in Figure 3. The geometry of the ground state of allene is known from electron diffraction studies,[29] and this structure and the predicted structures are also shown in Figure 3. Allene possesses D_{2d} symmetry, and thus three parameters uniquely define the molecular structure. The SCF bond lengths are slightly shorter than those from experiment as is typical of distances from the Hartree−Fock procedure. A higher level CCD/6-31G* optimization, which is also shown in Figure 1, more accurately describes the C=C bond length. The triplet

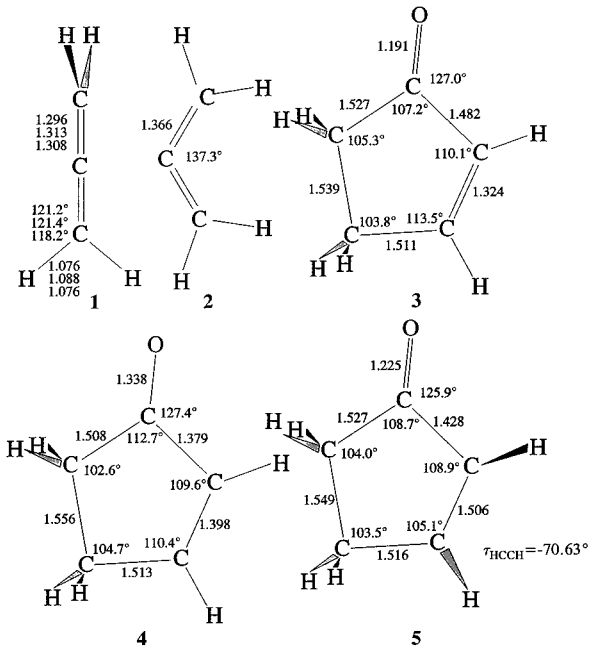

Figure 3. Important geometrical feature of the reactants: ground state allene (**1**), triplet excited state allene (**2**), ground state (**3**), and the $n \rightarrow \pi^*$ (**4**) and $\pi \rightarrow \pi^*$ (**5**) triplet states of cyclopentenone. Optimizations were carried out at the SCF/6-31G* level for all structures except allene (**1**) where the SCF/6-31G*, CCD/6-31G*, and experimental structures are given, respectively.

excited state is planar with C_{2v} symmetry, and the carbon skeleton, which is linear in the ground state, is decidedly bent to a CCC angle of 137.3°.

Ground state singlet cyclopentenone has a plane of symmetry[30] as does the $n \rightarrow \pi^*$ triplet species. In these two states, the two hydrogens attached to the initial double bond and the entire enone moiety are planar. In the π,π^* triplet state, these two hydrogens are twisted. The ground state carbonyl bond length of 1.19 Å lengthens to ∼1.34 Å in the $n \rightarrow \pi^*$ triplet or to ∼1.23 Å in the $\pi \rightarrow \pi^*$ triplet excited state. Both the C=C and C=O bond lengths in the excited state of cyclopentenone would be expected to be longer than in the ground state, as the π^* orbital which is populated upon excitation has nodes between these atoms. In contrast, the C−C bond between C=C and C=O should be slightly shorter, since there is a bonding interaction in the π^* orbital. The geometries of these three states of cyclopentenone are depicted in Figure 3.

In enone/alkene photochemical cycloaddition experiments, an excited enone is usually assumed to be one of the reactants. However, the lowest excited triplet state of allene at its relaxed geometry lies only 51.5 kcal/mol above its ground state. Thus, energy transfer from the excited triplet cyclopentenone (72.3 kcal/mol) to allene could allow access to lower energy transition states. This does not imply that the transition state barriers are lower than for triplet cyclopentenone plus singlet allene but rather that the whole potential energy surface is lower by a significant amount. The quantum chemical methods employed cannot be used rigorously to search large regions of the higher triplet potential energy surface of the same symmetry which lies ∼20 kcal/mol above the limit of triplet allene plus ground state cyclopentenone.

(27) (a) Furlani, T. R.; King, H. F. *J. Chem. Phys.* **1985**, *82*, 5577. (b) King, H. F.; Furlani, T. R. *J. Comput. Chem.* **1988**, *9*, 771. (c) Carlacci, L.; Doubleday, C., Jr.; Furlani, T. R.; King, H. F.; McIver, J. W., Jr. *J. Am. Chem. Soc.* **1987**, *109*, 5323.

(28) Arnaut, L. G.; Caldwell, R. A.; Elbert, J. E.; Melton, L. A. *Rev. Sci. Instrum.* **1992**, *63*, 5381.

(29) Ohshima, Y.; Yamamoto, S.; Nakata, M.; Kuchitsu, K. *J. Phys. Chem.* **1987**, *91*, 4696.

(30) Organ, M. G.; Froese, R. D. J.; Goddard, J. D.; Taylor, N. J.; Lange, G. L. *J. Am. Chem. Soc.* **1994**, *116*, 3312.

Table 1. Energetics of the Intermediates and Transition States Resulting from the Addition of the Allene and Cyclopentenone Systems[a]

	UHF//UHF	UMP2//UHF	UMP3//UHF	S^2	ZPVE	ΔE	min/TS
			Biradical **10**				
11	−383.514 235	−384.642 794	−384.702 804	2.24	103.7	25.8	min
12	−383.514 016	−384.643 427	−384.702 970	2.24	103.9	25.9	min
13	−383.511 766	−384.640 150	−384.700 139	2.24	103.6	27.4	min
14	−383.508 935	−384.637 808	−384.697 985	2.24	103.7	28.8	TS (**11-13**)
15	−383.507 295	−384.636 847	−384.696 826	2.24	103.8	29.6	TS (**11-12**)
16	−383.502 950	−384.632 342	−384.692 118	2.24	103.7	32.5	TS (**12-13**)
17	−383.467 884	−384.601 020	−384.660 393	2.30	101.9	50.6	TS (reactants-**11**)
18	−383.468 187	−384.603 300	−384.662 163	2.29	102.1	49.7	TS (reactants-**12**)
19	−383.466 513	−384.599 743	−384.658 970	2.31	101.9	51.5	TS (reactants-**13**)
			Biradical **20**				
21	−383.546 596	−384.676 185	−384.735 451	2.23	103.1	4.7	min
22	−383.542 980	−384.673 303	−384.732 573	2.23	103.4	6.8	TS (**21**−**21**)
23	−383.488 898	−384.614 004	−384.674 917	2.43	101.4	41.0	TS (reactants−**21**)
			Biradical **30**				
31	−383.526 217	−384.644 739	−384.708 838	2.36	104.4	22.7	min
32	−383.525 326	−384.645 169	−384.708 900	2.36	104.4	22.7	min
33	−383.526 030	−384.644 448	−384.708 543	2.36	104.4	22.9	min
34	−383.517 620	−384.637 657	−384.701 471	2.35	104.4	27.3	TS (**31**−**32**)
35	−383.519 449	−384.638 583	−384.702 805	2.35	104.3	26.4	TS (**31**−**33**)
36	−383.517 500	−384.637 859	−384.701 743	2.35	104.4	27.1	TS (**32**−**33**)
37	−383.471 804	−384.598 467	−384.660 093	2.40	102.0	50.9	TS (reactants−**31**)
38	−383.471 504	−384.599 296	−384.660 644	2.39	102.1	50.6	TS (reactants−**32**)
39	−383.472 473	−384.599 470	−384.660 923	2.40	102.1	50.5	TS (reactants−**33**)
			Biradical **40**				
41	−383.557 935	−384.677 399	−384.741 175	2.35	103.7	1.7	min
42	−383.561 397	−384.680 290	−384.743 893	2.35	103.7	0.0	min
43	−383.557 917	−384.677 314	−384.741 060	2.35	103.7	1.8	TS (**41**−**42**)
44	−383.557 291	−384.676 406	−384.740 414	2.36	103.7	2.2	TS (**41**−**42**)
45	−383.490 080	−384.610 949	−384.673 355	2.46	101.4	42.0	TS (reactants−**41**)
46	−383.490 077	−384.610 998	−384.673 391	2.46	101.4	41.9	TS (reactants−**42**)

[a] Energies are from HF, MP2, and MP3 levels at the fully optimized SCF/6-31G* geometry. Energy differences relative to biradical **42** are in kcal/mol at the MP3//SCF + ΔZPVE level. The S^2 value and the nature of the stationary point are also listed. The relative energy of the reactants (triplet allene plus singlet cyclopentenone) is 32.8 kcal/mol with respect to **42**.

Table 2. Energetics of the Reactants and Products in the Allene Plus Cyclopentenone Cycloaddition[a]

compound[b]	HF//HF	MP2//HF	MP3//HF	S^2	ZPVE	ΔE
1	−115.861 101	−116.233 079	−116.257 627	0.00	37.3	
2	−115.815 947	−116.140 712	−116.171 805	2.13	34.9	
3	−267.685 393	−268.486 710	−268.515 864	0.00	66.3	
4	−267.611 101	−268.345 619	−268.392 848	2.20	63.4	
5	−267.607 445	−268.354 115	−268.395 913	2.15	63.3	
1 + **3**	−383.546 494	−384.719 789	−384.773 491	0.00	103.6	−18.7
2 + **3**	−383.501 340	−384.627 422	−384.687 669	2.13	101.2	32.8
1 + **4**	−383.472 202	−384.578 698	−384.650 475	2.20	100.7	55.6
1 + **5**	−383.468 546	−384.587 194	−384.653 540	2.15	100.6	53.6
HH	−383.583 197	−384.776 837	−384.823 837	0.00	108.5	−45.4
HT	−383.583 619	−384.776 314	−384.824 249	0.00	108.5	−45.6

[a] The energies are from HF, MP2, and MP3 levels at the fully optimized SCF/6-31G* geometries. Energy differences (ΔE) relative to compound **42** are in kcal/mol at the MP3//SCF + ΔZPVE level. The total energies of **42** are given in Table 1. The S^2 values are also tabulated. [b] See Figure 3 for **1**, **2**, **3**, **4**, and **5**.

In the 1,4-biradical trapping experiments, the details of the formation of the biradicals are not known. The transition states (from reactants) considered in the following discussions lead from the lowest triplet excited state of allene and ground state cyclopentenone to the triplet 1,4-biradical minima. Clearly the triplet energy of allene is not very high, and indeed we have computational evidence that the relaxed triplet energies of many alkenes are not as high as previously thought.[31] Thus, thermodynamics would allow triplet energy transfer to the allene from cyclopentenone, although the dynamics of such a process have not been examined by us.

Regioisomers. The reaction of allene with cyclopentenone previously has been studied in detail, and these experimental results are summarized in Figure 1.[20] Weedon has suggested that only three of the metastable biradicals were formed, and only two (**10** and **20**) in appreciable amounts. The UHF, UMP2, and UMP3 6-31G* energies of the triplet transition states leading from excited state reactants to the triplet biradical minima, the minima themselves, and the transition states for internal rotation between triplet minima are listed in Table 1. Table 2 presents energies for the reactants both as individual species (e.g., **1**) and on pairs of reactants (e.g., **1** + **3**), and for the head-to-head and head-to-tail cycloadducts formed in the reaction.

Four different 1,4-biradical isomers could result from the cyclopentenone−allene photoaddition. Biradicals **10** involve addition α to the carbonyl to one of the terminal carbons of allene. Biradicals **20** also resulted from α

(31) Froese, R. D. J.; Lange, G. L.; Goddard, J. D. Submitted for publication in *J. Am. Chem. Soc.*

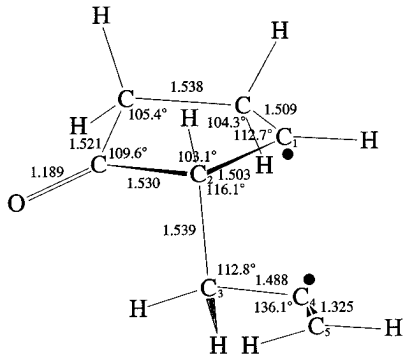

Figure 4. Geometrical features of the lowest energy conformation of the set of biradicals **10**. This species, **11**, was optimized at the SCF/6-31G* level of theory. The distance between radical sites C_1 and C_4 which carry most of the radical character is 3.148 Å, and the $C_1-C_2-C_3-C_4$ torsional angle is 293.8°.

addition, but to the central carbon of allene. Biradicals **30** and **40** both resulted from β addition, with **30** at the terminal and **40** at the central carbon of allene. The energetics of these systems will be discussed in detail.

Much of the discussion in this paper concerns "radical sites". For the unrestricted Hartree−Fock procedure, the atomic spin densities on the radicals have been examined to estimate the location of most of the spin density. For **10**, the radical sites as depicted in Figure 1 have spin density values of 1.248 (C in the ring) and 1.625 (C in the allene moiety). For **30**, these values are 1.095 and 1.628. For the allylic-substituted species **20**, the ring carbon has a spin density value of 1.236, and both terminal allyl carbons have substantial contributions of 1.032 and 1.024. In compound **40**, the ring carbon has a spin density of 1.089, and the two carbons in the allene component of the molecule have values of 1.000 and 1.048. In a simplified model, discussions often refer to the distance between the radicals as if the spins were localized on those carbons for which the largest spin density values were found.

Biradicals 10. There are three triplet 1,4-biradical minima associated with the overall structure **10**. Figure 4 shows the structure of the lowest energy conformer, **11**. As the $C_1-C_2-C_3-C_4$ torsional angle τ is varied from 0° to 360°, three different minima and the corresponding internal rotation transition states were located. The energetics of the minima and transition states are shown schematically in Figure 5. The dihedral angle τ varies from 54.4° (minimum **12**) to 121.0° (TS **16**) to 189.9° (minimum **13**) to 235.8° (TS **14**) to 293.8° (minimum **11**) to 355.8° (TS **15**) and back to 54.4° (minimum **12**). As with the rotation of a methyl group in ethane, the minima are separated by a torsional angle of approximately 120° when considered as Newman projections. In this and other schematic potential energy surface drawings (Figures 5, 7, 9, and 11), the free energies ($\Delta G = \Delta H - T\Delta S$, where $\Delta H = \Delta E$ since there are no ΔnRT terms in these cases) are plotted. The discussions in the text unless otherwise stated refer to ΔE (UMP3//HF + ΔZPVE). Energies quoted in Tables 1 and 2 are relative to the lowest energy intermediate biradical, **42**.

Structures **11** and **12** are almost equi-energetic, differing by ~0.1 kcal/mol. The third minimum in this group, **13**, lies 1.6 kcal/mol above **11**. The internal rotation has barriers which range from 1.4 to 6.6 kcal/mol. If the group is viewed as nearly freely rotating

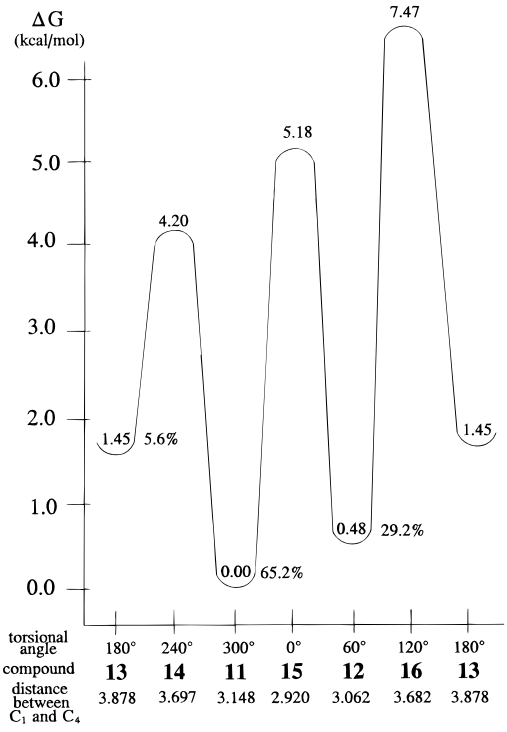

Figure 5. The nearly free rotation of the biradicals **10** through 360°. Free energy predictions, ΔG, were determined at the UMP3/6-31G* level. The relative populations were determined from theoretically predicted equilibrium constants.

about the C_2-C_3 bond, the relative populations of the various minima can be estimated thermodynamically. The ΔG values give these relative populations assuming the transition states are relatively low in energy and thus easily overcome. As indicated in Figure 5, the two radical bearing carbon centers are in close (within 3.2 Å) proximity in 94% (65% + 29%) of the conformations. The distances between carbons possessing most of the radical character also are shown in Figure 5.

In each of the three minima, the three substituents (C, H, H) in the allene fragment are staggered with respect to the C_2-H portion of the cyclopentenone ring. One of these conformations (**13**) results in the relatively close approach (3.106 Å) of C_4 to the carbonyl oxygen. From a qualitative viewpoint, this conformation would be higher in energy due to nonbonded repulsions, and this notion is supported quantitatively by the *ab initio* results.

Transition states were located which led from the triplet reactants to the three biradical minima. The $C_1-C_2-C_3-C_4$ torsional angle τ of the three transition states corresponds closely with the same angle in the minima. τ for **17** of 292.1° corresponds closely to that of **11** of 293.8°, and similarly the values for **18** of 49.8° (**12**, 54.4°) and **19** of 185.1° (**13**, 189.9°) are also close. The transition state barriers lead from triplet allene and singlet cyclopentenone, which have a combined energy relative to **42** of 32.8 kcal/mol. In comparing the three transition states, the differences between the various barrier heights are less than 2 kcal/mol. The lowest of the three transition states, **18**, presents an energetic barrier of 16.9 kcal/mol relative to the specified reactants.

The geometry of the allene moiety of the biradical minima is important to later comparisons. For the lowest energy biradical resembling **10**, the potential energy surface leads from reactants through transition state **17**

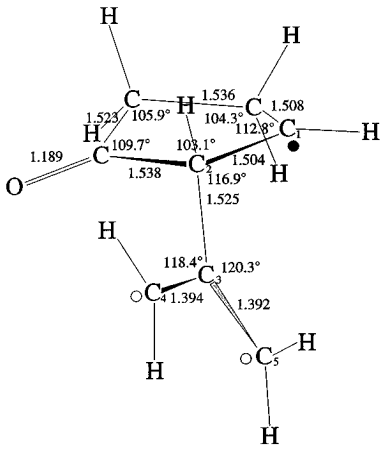

Figure 6. Geometrical features of the lowest energy conformation of the biradicals **20**. This species, **21**, was optimized at the SCF 6-31G* level of theory. The distances from C_1 to the allyl sites C_4 and C_5 are 3.804 and 2.978 Å, respectively.

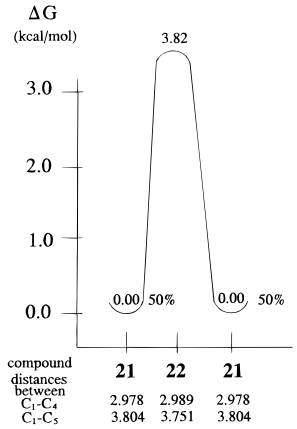

Figure 7. Rotation of biradicals **20** through 180°. Free energy predictions, ΔG, were determined at the UMP3/6-31G* level. The relative populations were determined from theoretically predicted equilibrium constants.

to biradical minimum **11**, and the C_3-C_4 and C_4-C_5 bond lengths can be examined. These bond lengths which are both equal at 1.366 Å in triplet allene, change to 1.314 and 1.441 Å in **17** and are 1.325 and 1.488 Å in **11**. Clearly, the allene part of the minimum possesses one single and one double bond. The lengths of the bonds which are formed in the transition states are especially interesting. The C_2-C_3 bond lengths in the three transition states are very similar at 2.100 (**17**), 2.095 (**18**), and 2.094 Å (**19**). These bonds shorten to lengths of 1.539 (**11**), 1.542 (**12**), and 1.539 Å (**13**), in the respective minima. For the three transition states, the distances between the centers formally having the radicals are 3.385 (**17**), 3.346 (**18**), and 4.021 Å (**19**), and they parallel the trends observed for the triplet 1,4-biradical minima (**11** to **13**).

Biradicals 20. In the addition of the central carbon of allene to cyclopentenone (at the position α to the carbonyl), a substituted allyl radical is formed. **21** is the lowest energy minimum of this type. Unlike the biradicals such as **10** which may be viewed as having sp^3 hybridization at C_3 and have three minima connected by internal rotation, the allyl radicals with what would be considered as sp^2 hybridization at C_3 have two shallow rotational minima separated by a torsional angle of approximately 180°. In fact, these two minima are identical (**21**) with the terminal carbons reversed due to the rotation by 180°. In addition, there are two identical transition states (**22**), formed by rotating approximately 90° from either minimum.

The minimum energy structure, **21**, is shown in Figure 6. Note that the two bonds in the allyl fragment are approximately equal at 1.394 (C_3-C_4) and 1.392 Å (C_3-C_5). Our results indicate that both of the exterior carbons possess radical character and both C−C bonds are delocalized. This fact clearly contrasts with radicals like **10** where essentially a single bond and a double bond were evident. As Table 1 indicates, there is significant stabilization by the allyl type radical, as the energy of **21** is 21.1 kcal/mol lower than that of **11** (UMP3//SCF + ΔZPVE).

Rotation about the C_2-C_3 bond results in identical minima separated by 180°. Carbon 3 in the biradicals **20** may be considered to be sp^2 hybridized; thus, two minima are expected. In contrast, C_3 for biradicals such as **10** can be viewed as sp^3 hybridized; thus, there are three minima. Predictions derived from Table 1 show that the minimum is 2.1 kcal/mol in energy below the transition state. However, the radical character on the terminal carbons ensures that these two radical sites are always somewhat close, and products could form upon spin inversion. The distance between the radicals in the transition state is 2.989 Å. Note also that the hydrogen attached to carbon 1 is nearly planar relative to the adjacent carbons supporting the view of the sp^2 nature of the radical-bearing carbon in the cyclopentenone ring. In fact, for all of the biradical minima examined in this study, the hydrogen at the radical site on the ring is nearly planar with respect to the two adjacent carbons.

The one transition state, **23**, leading from excited state reactants to biradical **21** has a barrier of 8.2 kcal/mol. The stability of the 1,4-biradical minimum is reflected in the transition state energy as this particular barrier is the lowest in energy of all the transition states found leading from the reactants. The C_2-C_3 bond distance of 2.251 Å in **23** is quite long indicating an early transition state and suggesting a relatively small barrier. The central carbon (C_3) of the allene moiety adds from directly above the carbon (C_2) in the cyclopentenone ring. Transition state **23** is ∼8.7 kcal/mol lower in energy than **18**, which is the lowest energy transition state leading to the other biradicals **10**.

Biradicals 30. Similar to the case of the biradicals **10**, there are three metastable triplet 1,4-biradical minima associated with β-addition. These are formed upon the addition of allene (terminal carbon) to the β-position of the enone. Figure 8 depicts the lowest energy form of these three conformers, **31**. As the $C_1-C_2-C_3-C_4$ torsional angle τ is varied between 0° and 360°, three different minima and the corresponding transition states were located. The dihedral angle τ varied from −0.1° or +359.9° (TS **34**) to 60.9° (min **32**) to 120.4° (TS **36**) to 183.2° (min **33**) to 239.4° (TS **35**) to 296.2° (min **31**) and back to −0.1° (TS **34**). Schematically, the energetics of the minima and transition states are shown in Figure 9.

Structures **31** and **32** are essentially equal in energy. The third minimum in the group, **33**, lies only 0.2 kcal/mol above the other two. Overall, the energies of these triplet 1,4-biradicals **30** are lower than the biradicals **10** by approximately 3 kcal/mol. This small extra stabilization may be due to one of the radical centers being adjacent to the carbonyl group. However, the allylic type radicals **20** are more stable than **30** by about 18 kcal/

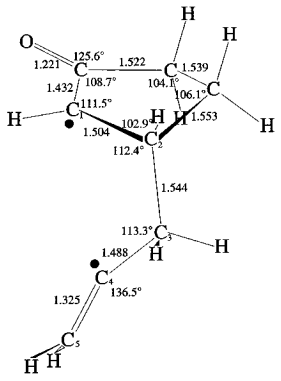

Figure 8. Geometrical features of one of the lowest energy conformations of the biradicals **30** This species, **31**, was optimized at the SCF 6-31G* level of theory. The distance between sites C_1 and C_4 is 3.072 Å, and the $C_1-C_2-C_3-C_4$ torsional angle is 296.2°.

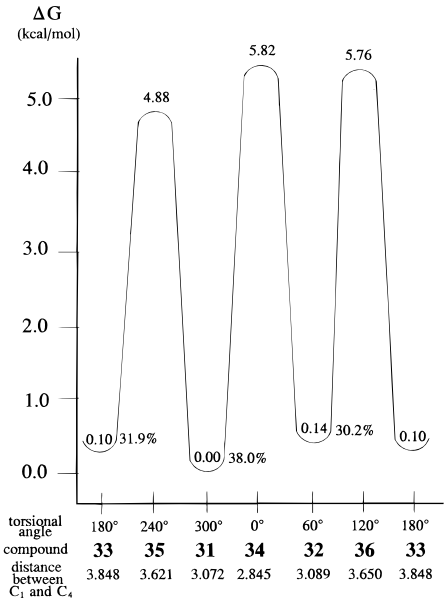

Figure 9. The nearly free rotation of biradicals **30** through 360°. Free energy predictions, Δ*G*, were determined at the UMP3/6-31G* level. The relative populations were determined from theoretically predicted equilibrium constants.

mol. Barriers to internal rotation for **30** about the C_2-C_3 bond range from 3.5 to 4.6 kcal/mol. Figure 9 indicates that the two carbon centers formally carrying the radicals are relatively close to each other in approximately 68% (38% + 30%) of the conformations. The distances between the carbons labeled as possessing the radical character are shown in Figure 9 for each species.

Transition states from the triplet reactants to the three biradical minima were located. Once again, the $C_1-C_2-C_3-C_4$ torsional angle τ of the three transition state parallels this angle in the minima. τ for transition state **37** of 299.6° corresponds to the 296.2° for minimum **31**, τ for **38** of 70.8° compares closely with that for **32** of 60.9°, and the value for **39** of 182.5° parallels that for **33** of 183.2°. The difference between the barriers for these three transition states is less than 0.5 kcal/mol. The lowest energy barrier to forming biradicals **30** from reactants is 17.7 kcal/mol and involves transition state **39** to minimum **33**.

The geometry of the allene moiety in the biradical minima is similar to that in the biradicals **10**. The distances clearly suggest a single and a double bond. The

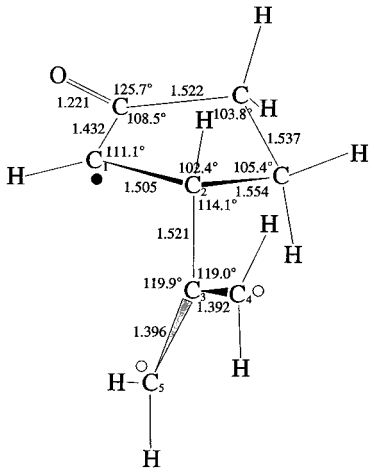

Figure 10. Geometrical features of the lowest energy conformation of the biradicals **40**. This species, **42**, was optimized at the SCF 6-31G* level of theory. The distances between C_1 and the allyl sites C_4 and C_5 are 3.742 and 3.018 Å, respectively.

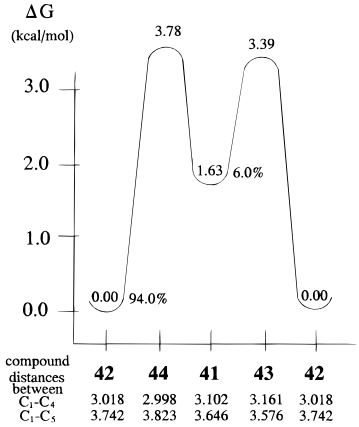

Figure 11. Rotation of biradicals **40** through 180°. Free energy predictions, Δ*G*, were determined at the UMP3/6-31G* level. The relative populations were determined from theoretically predicted equilibrium constants.

lengths of the bonds forming in the transition states are similar to those for biradicals **10**. The C_2-C_3 bond lengths in the three transition states are 2.150 (**37**), 2.147 (**38**), and 2.142 Å (**39**), which are shorter than the 2.251 Å bond length in **23**. These shorter bond lengths indicate a tighter transition state and qualitatively suggest a higher energy barrier.

Biradicals 40. There are two unique triplet 1,4-biradical minima related to **40**. Of the nine triplet biradical minima examined in this study, the biradicals which possess allyl type stabilization are lowest in energy. At the UMP3/6-31G*//SCF/6-31G* level of theory, the lowest energy species of the nine studied is **42**. Weedon[18] has indicated that this 1,4-biradical is not produced. A rotational conformer of **42**, **41** lies only 1.7 kcal/mol higher in energy. Key structural features of the lowest energy species, **42**, are given in Figure 10, while the conformational differences between **41** and **42**, and selected important geometrical parameters are shown in Figure 11. As mentioned earlier when examining the triplet biradicals **20**, there are large geometrical differences between **20** and **40** and between the biradicals **10** and **30** as seen in the two exterior bond lengths in the allene moiety of the molecule. For the two biradicals **40**, the bond lengths are 1.389 and 1.400 Å in **41** and 1.396

and 1.392 Å in **42**. However, in **10** and **30**, there is clearly a single and a double bond, rather than two partially conjugated double bonds.

Nearly free rotation about the biradical bond (the dihedral angle τ of **42** denoted by carbons $C_1-C_2-C_3-C_4$ in Figure 10) from 0° to 360° revealed four shallow minima (two of which are identical) with dihedral angles τ of 61.1° (**41**), 140.4° (**42**), 239.5° (**41**), and 318.9° (**42**). See the schematic potential energy surface in Figure 11. Two transition states, **43** and **44**, were located which join these shallow minima and have dihedral angles of 28.8° (**44**), 69.5° (**43**), 205.4° (**44**), and 249.4° (**43**). The energetics (ΔG) of these transition states are also illustrated in Figure 11.

The lowest energy barrier to formation is 9.1 kcal/mol and involves transition state **46**, which leads from the reactants to the biradical minimum **42**. As in the allyl stabilization of **20**, both minima and transition states are stabilized considerably relative to **10** and **30**. The radical at the C_1 center is also stabilized slightly by the presence of the carbonyl group, and thus the biradical minimum of **40** is lower in energy than that of **20**.

Energy and Entropy Comparisons. Predictions of the relative energies of all the intermediate species at the UHF, UMP2, and UMP3 levels of theory are given in Table 1. The values of S^2 deviate from the ideal value for a triplet of 2.00 by nearly 25% in some cases (e.g., $S^2 = 2.46$ for **45** and **46**); thus, spin-projected MP2 (PMP2) values also were examined. The energy differences between the lowest energy species (**42**) and the other biradicals increased at this level of theory (PMP2 versus UMP2). At the PMP2 + ΔZPVE level, **42** is more stable than the following (kcal/mol): **11** by 29.6, **21** by 6.6, and **31** by 24.5 kcal/mol. In comparison at the UMP2 + ΔZPVE level, the same species, **42**, is more stable than **11** by 23.5, **21** by 2.0, and **31** by 23.0 kcal/mol. Energetically, the most stable species (**42**) was lowered by 3−6 kcal/mol relative to the other biradicals on going from the UMP2 to the PMP2 level of theory.

The energies within a set of biradicals change little at the PMP2 level. As an example, consider the 1,4-biradical minimum **10**. The species with the carbon centers formally being the unpaired spins as furthest apart is **13**, and at the UMP2 + ΔZPVE level, it lies 1.6 kcal/mol above **11**. At the PMP2 + ΔZPVE level, **13** is 1.4 kcal/mol above **11**. These numbers seem to indicate that despite some spin contamination, the UMP3 level is appropriate for comparisons in this study.

There are variations in the entropy values used in the free energy (ΔG) calculations. The absolute entropies for the species decrease in the following order: reactants > transition states leading from reactants > minima > internal rotation transition states. As would be anticipated, there is a larger difference between the reactants and any other species. There are much larger rotational and translational components of the entropy for the separated reactants.[32] The absolute entropy of the excited reactants (triplet allene with cyclopentenone) is 134.3 cal/(mol K), which can be compared with the value of 94.6 cal/(mol K), for **33**. In comparing transition states leading from reactants, minima, and rotational transition states, the difference arises from the vibrational contribution. The total entropies (cal/(mol K)), with vibrational contributions in brackets of **39**, **33**, and **35** are the following: **39**, 96.0 (24.3); **33**, 94.6 (23.0); **35**, 90.6 (18.8). The free energy predictions were used to calculate the fraction of molecules in the various internal rotation minima. These percentages for each of the radicals were presented in the figures.

(32) Hehre, W. J.; Radom, L.; Schleyer, P. v. R.; Pople, J. A. *Ab Initio Molecular Orbital Theory*; Wiley-Interscience: New York, 1986; p 251.

Table 3. Data on Factors Considered To Influence the Rate of Closure of the Triplet 1,4-Biradicals to Products

	R^a	%[b]	SOC[c]	S/T[d]	reverse barrier[e]
11	3.148	65.2	9.026	0.94	24.8
12	3.062	29.2	6.519	0.80	23.8
13	3.878	5.6	9.780	0.70	24.1
21	2.978	100.0	1.725	0.53	36.3
31	3.072	38.0	40.144	0.77	28.2
32	3.089	30.2	40.155	0.26	27.9
33	3.848	31.8	40.246	1.27	27.6
41	3.018	94.0	40.155	-0.53	40.3
42	3.102	6.0	40.186	-0.32	41.9

[a] Distance (Å) between the two carbons carrying most of the radical spin density. [b] Percentage of each radical (see Figures 5, 7, 9, and 11) on the basis of free energy predictions. [c] One-electron component of the spin−orbit coupling constant derived from a CAS(10,10)/6-31G calculation. Predicted values are in wavenumbers. [d] Singlet/triplet energy difference using a CAS(10,10)/6-31G wave function. Difference is E(singlet) − E(triplet) in kcal/mol. [e] Reverse barrier on the triplet potential energy surface from the respective 1,4-biradical minimum back to starting material at the UMP3//SCF + ΔZPVE level.

Spin−Orbit Coupling and Singlet−Triplet Energy Differences. Spin−orbit coupling (SOC) predictions were made for the triplet 1,4-biradical minima using the CAS-SCF method and the unpolarized 6-31G basis set. The complete active space was varied from a 2-electron, 2-orbital space to a 10-electron, 10-orbital space. The magnitudes of the constants vary depending on the size of the active space, but the relative values remain consistent. These coupling constants consider only the one-electron contribution, but once again on the basis of an earlier study,[27] the ordering would not be expected to change if the two-electron component was included.

Spin−orbit couplings could lead to an intersystem crossing anywhere in space where the singlet and triplet potential energy surfaces are close in energy. We have chosen to consider those regions of space containing minimum energy intermediates as probably most important in the intersystem crossing process due to the greater lifetime of such minima as compared to arbitrary regions of a potential energy surface.

As the CAS(10,10)/6-31G numbers collected in Table 3 indicate, addition β to the carbonyl enhances spin−orbit coupling quite dramatically. The overall SOC constants were approximately 40 cm^{-1} for both **30** and **40**. These values are significantly greater than those of 9.0, 6.5, and 9.8 cm^{-1} for **11**, **12**, and **13**, respectively, and of 1.7 cm^{-1} for **21**. The biradical, **13**, with the two formal radical centers furthest apart has the largest coupling constant of the group **10**, and this larger value would increase the likelihood of an intersystem crossing. However, **13** is the least stable of the three conformers of **10** and would not be present to as great an extent. Spin−orbit coupling for the allylic-substituted system **20** is extremely small with a magnitude of only ~1.7 cm^{-1}. The SOC values for this allyl-substituted system are less than those for **10** at all levels of theory [CAS(2,2) to CAS(10,10)]. This fact is somewhat surprising since Furlani and King have suggested[27] that systems with more radical character in the singlet state would possess larger spin−orbit coupling constants.

The spin−orbit coupling constants for the α-carbonyl radicals (**10**, **20**) are considerably smaller than for the β-carbonyl species (**30**, **40**). Because 97% of the intermediates trapped experimentally result from α-addition, one possibility could be that the larger spin−orbit coupling constant for the β-species results in too short-lived an intermediate that reverts to starting material before trapping could occur.

For the 1,4-biradicals, the energy differences between singlet and triplet states were determined by examining the CAS(10,10)/6-31G energies of both states. These energy gaps are important in various models for intersystem crossing[33] which would occur most efficiently for systems with very small singlet/triplet gaps. For biradicals **10**, the difference in the singlet/triplet splitting for the three minima is small, with the triplet state lower in energy in all cases. These gaps (kcal/mol) are 0.70 for **13**, 0.80 for **12**, and 0.94 for **11**. The smallest gap occurs for **13**, where the two radical centers are separated by 3.878 Å, but at this distance, cycloadducts are unlikely to form. The singlet/triplet gap for **21** is small at 0.53 kcal/mol. For the three 1,4-biradicals **30**, the singlet/triplet splittings range from 0.26 kcal/mol (**32** with a radical distance of 3.089 Å) to 0.77 kcal/mol (**31** with a radical distance of 3.072 Å) to 1.27 kcal/mol (**33** with a radical distance of 3.848 Å). Of these systems, the one least likely to cross from the triplet to the singlet potential energy surface due to a larger energy gap is **33** and this species has a large distance between the radical sites. At the CAS(10,10)/6-31G level of theory, the singlet states of radicals **41** and **42** are lower in energy than their triplet counterparts by 0.53 and 0.32 kcal/mol. The singlet/triplet gaps are all relatively small, and this factor is likely less important than are other considerations.

Predictions of Biradical Formation. In prediction of which 1,4-biradicals will be formed, transition state energies must be considered. As discussed earlier, in our calculations the transition states leading from reactants involve a triplet excited state allene and a ground state cyclopentenone. The lowest energy transition states correspond to the lowest energy 1,4-biradical minima, the allyl-substituted systems. The lowest energy transition state barriers for formation from reactants for each of the four biradical systems are 16.9 (**18**), 8.2 (**23**), 17.7 (**39**), and 9.1 kcal/mol (**46**). The barriers are relatively low suggesting early transition states according to the Hammond postulate for exothermic processes. The long C−C bond distance as the allene moiety attacks cyclopentenone also suggests an early transition state. The transition state energetics do not agree with the interpretations of experimental data by Weedon.[18] Our theoretical predictions suggest that the two allyl-substituted systems should form most, if not all, of the 1,4-biradical intermediates. We predict that the four 1,4-biradicals **10**:**20**:**30**:**40** would form in a ratio of 0:83:0:17.

The transition state energies considered here (triplet excited state allene with ground state cyclopentenone) are lower than those involving excited state cyclopentenone and ground state allene. Excited state cyclopentenone reacting with ground state allene (Table 2, **1** + **4**) lies 20.8 kcal/mol above the excited state allene plus ground state cyclopentenone (**2** + **3**) combination. Thus, any transition states with a barrier leading from allene plus triplet cyclopentenone would be on a higher potential energy surface by at least this 20.8 kcal/mol. The barriers through transition states **23**, **45**, and **46** are 8.2, 9.2, and 9.1 kcal/mol, respectively, and are probably not in a region of intersection with the next excited surface. In fact, the highest barrier from reactants in this study leading from reactants was 18.7 kcal/mol via **19**. These energies must be overall lower than the transition states leading from the singlet allene plus triplet cyclopentenone limit since the transition state energies are below that of the singlet allene/triplet cyclopentenone limit. The transition state energies across the triplet allene/singlet cyclopentenone are lower in energy, but this does not imply that this mechanism is followed in the experiment where excess energy is available through the photoexcitation. These triplet allene transition states may be lower in energy, but it is still possible that transition states in very different regions of the surfaces are involved in the formation of the biradicals. Triplet−triplet energy transfer would be required, and even though the relaxed triplet of allene lies 20.8 kcal/mol below the relaxed triplet of cyclopentenone, the MP3//SCF vertical excitation energy of allene (singlet−triplet energy difference at the singlet geometry) is 117.8 kcal/mol. This prediction is in accord with the experimental photoelectron spectra values for the lowest two triplet states of ∼98.7 and 112.8 kcal/mol.[34] Allene gains considerable stability through geometrical relaxation. Even though triplet−triplet energy transfer may seem unlikely due to the very different vertical and relaxed geometries, there is theoretical evidence that such non-vertical transfer can occur in enone−alkene systems.[31]

If the transition states leading from triplet allene and singlet cyclopentenone are not accessed experimentally, can anything be said about the transition states leading from singlet allene and triplet cyclopentenone? The stability of the 1,4-biradicals corresponded to the stability of the transition states for triplet allene plus singlet cyclopentenone; i.e., the allylic intermediates were most stable, and the allylic transition states were most stable. Hence, it is possible that for the transition states for singlet allene plus triplet cyclopentenone leading to the 1,4-biradicals, the ordering still may be the same as in the case considered explicitly in our calculations, with the allylic transition states lowest in energy.

Predictions of Product Formation from the 1,4-Biradicals. If the yields of the 1,4-biradicals were known, then the relative amounts of products could be estimated. Table 3 lists potentially important factors such as the distance between the carbon centers with greatest spin density, the percentage of each biradical conformer on the basis of the free energy predictions, the one-electron spin−orbit coupling constants, the singlet−triplet energy gaps, and the reverse barriers to form excited triplet reactants. It is impossible to quantitatively estimate the amounts of products since all these factors play a role, but the weight to give to each factor is unknown.

The large difference in the spin−orbit coupling constants for the different biradicals is important. Biradicals **10** have a relatively small coupling constant; thus, an intersystem crossing to the singlet surface may have a low probability. The reverse barrier across the triplet

(33) (a) Landau, L. *Phys. Z. Sowjetunion 2* **1932**, 45. (b) Zener, C. *Proc. R. Soc. London* **1933**, *A137*, 696. (c) Zener, C. *Proc. R. Soc. London* **1933**, *A140*, 660.

(34) Mosher, O. A.; Flicker, W. M.; Kuppermann, A. *J. Chem. Phys.* **1975**, *62*, 2600.

transition states is moderate at approximately 24 kcal/mol, and this could lead to either ground (by an intersystem crossing) or excited state reactants. The ground state reactants could be excited once again to form triplet biradicals. A large percentage of these triplet biradicals might be expected to revert to starting material.

The spin−orbit coupling constant for **21** is extremely small, but in contrast to **10**, the reverse barrier for **20** is larger, and this reversion is much less likely. Thus, even though the spin−orbit factors do not favor spin inversion for **20**, the large reversion barrier leaves spin inversion of the biradical as the one way out. The relatively short distance between the two radical sites allows closure to head-to-head cycloadduct once spin inversion has occurred.

For biradicals **30**, the SOC constant is quite large for all three conformations; thus, spin inversion may be probable. One conformation has a relatively large singlet/triplet gap (1.27 kcal/mol), that being the conformation with the radicals furthest apart. Since the three biradical minima exist in approximately equal amounts (**31** 38%, **32** 30%, **33** 32%) and the conformation with the long distance between the radicals (**33**) has a large singlet/triplet gap, this would suggest that a large fraction of these biradicals will close to cycloadducts. Favorable spin−orbit interactions may not allow the reverse reaction path on the triplet potential energy surface to be followed.

For biradicals **40**, the SOC constant is relatively large for both conformations. All internal rotations leave the two radical sites relatively close. Unlike the other three types of systems, biradical **40** has the singlet potential energy surface lower in energy than the triplet surface. For these species, the reverse barrier is very large at over 40 kcal/mol; thus, spin inversion most likely occurs. It would be predicted that almost all of these species would close to the head-to-tail products.

To summarize, we estimate that **10** does not close efficiently, while **20**, **30**, and **40** all do. Given the information in Table 3, we could estimate somewhat arbitrarily the relative efficiency of ring closure: **10**, 10%; **20**, 80%; **30**, 80%; **40**, 100%. The predictions of the efficiencies of ring closure of these four biradicals can now be combined with the predictions of formation of the 1,4-biradicals. From our biradical predictions for **10**:**20**:**30**:**40** of 0:83:0:17, a ratio of 80:20 HH:HT is estimated. Bauslaugh's concept[35] that the more stable biradicals might revert to starting materials gains some plausibility from our results. In this case, stability does not necessarily refer to thermodynamic stability but to lack of ability to undergo an intersystem crossing when the 1,4-biradicals are formed.

Conclusions

The photochemical addition of triplet allene to singlet cyclopentenone has been studied theoretically. The excited triplet state of allene was determined to be 20.8 kcal/mol lower than the $\pi \rightarrow \pi^*$ triplet state of cyclopentenone. In our model where the reaction occurs by interaction of the relaxed triplet excited state of allene with ground state cyclopentenone, transition states were located leading from the overall excited triplet reactants to four different 1,4-biradicals. The two biradicals with allylic stabilization were significantly lower in energy. The transition state involving an allyl group attacking β to the carbonyl (**20**) was lowest in energy. Free energy predictions indicate that these two allyl-substituted 1,4-biradicals would form in a 83:17 ratio (β-**40**:α-**20**). Our theoretical predictions for the ratio of formation of the biradicals differ from the values obtained in trapping experiments.[18]

Internal rotational transition states and minima were determined for four 1,4-biradicals to predict which conformations were most probable. The two most important biradicals, **10** and **20**, both have very small spin−orbit coupling constants, but the reverse barrier to lead back to reactants from **10** is predicted to be 10 kcal/mol lower in energy than that leading back from **20**. Thus, Bauslaugh's hypothesis regarding stable biradicals reverting back to starting material might be valid. Our theoretical results indicate clearly that the importance of another reaction of the triplet 1,4-biradicals, i.e., reversion to reactants by triplet transition states, should be considered.

Acknowledgment. The Natural Sciences and Engineering Research Council of Canada (NSERC) is acknowledged for support in the form of a postgraduate scholarship (R.D.J.F.) and research grants (J.D.G. and G.L.L).

JO9514026

(35) Bauslaugh, P. G. *Synthesis* **1970**, 287.